An Expanded IrO$_2$/Ti Durable Electrode for Electrochemical Degradation of Basic Red 46 Textile Dye in Both Single and Binary Mixture Solutions

Raghda M. Belal · Mohamed A. Zayed · Nabil A. Abdel Ghany

Abstract The use of dimensionally stable anode (DSA) for degrading organic pollutants is of concern recently. The electrocatalytic technique can efficiently treat biodegradable organic matter like dye-containing effluent discharge. This study focuses on applying modified DSA meshed IrO$_2$/Ti electrode for the electrochemical degradation of wastewater effluents of Basic Red 46 (BR46) textile dye using different supporting electrolytes; sodium sulfate (Na$_2$SO$_4$) or/ and sodium chloride (NaCl). The parameters affecting the proposed electrochemical degradation process were evaluated to select the optimal operating conditions. The results revealed that using a mixture of supporting electrolyte Na$_2$SO$_4$ and NaCl enhanced the removal of dye color %, chemical oxygen demand (COD) %, and total organic carbon (TOC) % by 94.9%, 65.7%, and 76.0%, respectively. The UV-Vis and FT-IR spectroscopic techniques followed the degradation efficiency. FT-IR data were in good agreement with the COD, TOC, and UV-Vis measurements, confirming the high refractory performance of the BR46 dye. The redox process was performed on the surface of the modified electrode and explained via cyclic voltammetry (CV), and it showed a diffusion mass transport mechanism followed by product adsorption. The identification of the degradation products was assessed by gas chromatography–mass spectrometry (GC-MS) analysis. The electrochemical degradation and mineralization of a binary mixture of Basic Yellow (BY28) and BR46 textile dyes were also studied. It gave similar degradation and mineralization behavior to the same extent as the single dye in solutions.

R. M. Belal · M. A. Zayed
Chemistry Department, Faculty of Science, Cairo University, Giza 12613, Egypt

R. M. Belal
Basic Science Department, Modern Academy for Engineering and Technology, Maadi, Cairo, Egypt

N. A. A. Ghany (✉)
Physical Chemistry Department, Electrochemistry and Corrosion Lab., National Research Centre, Cairo 12622, Egypt
e-mail: na.abdelghany@nrc.sci.eg; na_manakhly@yahoo.co.uk

1 Introduction

The pollutant discharge of dye-containing effluent from textile industries is one of the most severe environmental concerns (Ali et al., 2005; Eswaramoorthi et al., 2008; Ghaly et al., 2014; Talukdar, 2001; Lima et al., 2007; Mathur et al., 2005; Morikawa et al., 1997; Nilsson et al., 1993; Tüfekci et al., 2007). Recently, many efforts have been directed toward the remediation of these dye effluents by newly proposed

methods. Generally, dye removal and decolorization have three main categories, and each method has its advantages and demerits. These categories are physical (Bogoeva-Gaceva et al., 2008; Farhadian et al., 2015; Rahman, 2016; Rajabi et al., 2016; Regti et al., 2017), biological (Aksu, 2005; Oliveira et al., 2007; Frijters et al., 2006; Santos et al., 2007; Torres et al., 2003), and chemical (Azbar et al., 2004; Ghoreishi & Haghighi, 2003; Gomes De Moraes et al., 2000; Keshmirizadeh & Farajikhajehghiasi, 2014; Nam & Tratnyek, 2000; Zaharia et al., 2009). Physical methods suffer some problems like excess sludge production and solid adsorbent disposal. Its efficiency increases only when the effluent volume is small. Biological treatment is based on aerobic and anaerobic degradation by microorganisms like fungi and bacteria. Sometimes biological methods alone are insufficient because the dye molecule structure may be non-biodegradable. Chemical oxidations have low efficiencies and need transportation and storage of dangerous reactants. Electrochemical oxidation techniques offer industrial activities an alternative solution to many environmental problems (Aquino et al., 2011; Fil & Günaslan, 2022, 2023; Fil et al., 2022; Körbahti & Tanyolac, 2008; Sanroman et al., 2004; Singh et al., 2013; Tsantaki et al., 2012; Uliana et al., 2012). This technique provides an easily automatable, versatile, cost-effective, efficient, and clean reagent because it depends on electrons to degrade the organic matter (Panizza & Cerisola, 2009). The selection of anode base metal for a given electrochemical treatment requires achieving significant efficiency in organic pollutant degradation, high stability under anodic polarization, and low production costs (Santos et al., 2016). Therefore, a modified dimensionally stable anode (DSA) meshed IrO_2/Ti electrode as an anode was applied. This electrode has been applied in numerous industrial electrochemical processes such as chlorine-alkali and sulfuric acid (Cotillas et al., 2016; Massué et al., 2017). Besides, it had been used for the degradation of organic pollutants and dye effluents (Awad & Ghany, 2015; Belal et al., 2021, 2022; Wang et al., 2010; Yaqub et al., 2018; Zaviska et al., 2009). Among dye-containing effluent pollutants, Basic Red 46 (BR46) textile dye was selected (Bouafia-Chergui et al., 2012; Rasoulifard et al., 2011; Torres-Luna et al., 2019). It is mainly used in acrylic fiber and scattered dyeing wool. It also can be used for direct printing in wool, silk, acrylic,

and polyester textile printing ("Basic Red46", 2021). This work is focused on the electrochemical treatment of wastewater effluents of BR46 textile dye and its binary mixture with Basic Yellow 28 (BY28) textile dye, which have hazardous effects on the environment and human health. The mixed binary textile dyes have been chosen in order to simulate the real treatment of industrial wastewater effluents. The proposed electrochemical oxidation process was performed using modified DSA $Ti\text{-}IrO_2$ meshed electrode. Different supporting electrolytes of sodium sulfate (Na_2SO_4), sodium chloride (NaCl), and a mixture of ($Na_2SO_4 + NaCl$) were used and their influence on the efficiency of the proposed electrochemical treatment was considered as a point of concern. The optimum conditions controlling the electrochemical degradation of dyes such as pH, current density, electrode type material, initial dye concentration, and supporting electrolyte concentration were studied. The degradation efficiency of the proposed electrochemical technique was followed by UV-visible spectrophotometer (UV-Vis), Fourier transform infrared (FT-IR), and gas chromatography–mass spectrometry GC-MS analysis. The degree of decolorization and mineralization was demonstrated using chemical oxygen demand (COD) and total organic carbon (TOC) measurements. The corresponding current efficiency and energy consumption were also estimated to validate the proposed electrochemical method. Cyclic voltammetry (CV) measurements were used to describe the redox process of the proposed electrochemical technique.

2 Experimental

2.1 Chemicals and Materials

A cationic textile dye Basic Red 46 belongs to a single azo class (Aakar dyes and chemicals, India), with molecular formula $C_{18}H_{21}BrN_6$, Mwt = 401.3 g mol^{-1}, λ_{max} = 530 nm; the cited study also used Azomethine class, A cationic textile dye CI Basic Yellow 28 (BY28) (Aakar dyes and chemicals, India), with molecular formula $C_{21}H_{27}N_3O_5S$, Mwt = 433.5 g mol^{-1}, λ_{max} = 440 nm; and the molecular structure of BY28 and BR46 textile dyes are shown in Fig. 1.
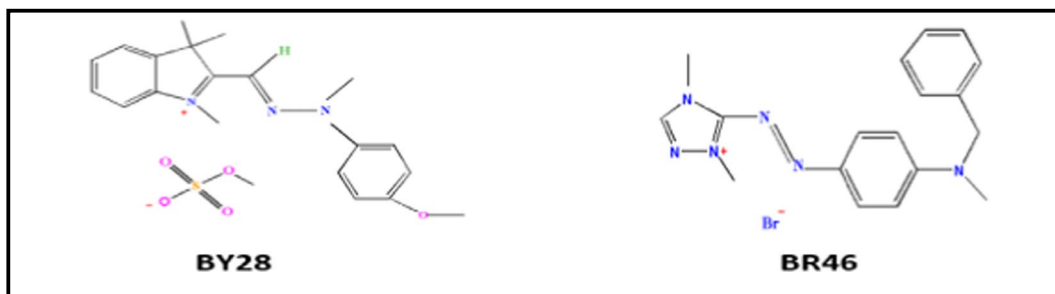
Fig. 1 Chemical structure of BY28 and BR46 dyes

A stock solution of supporting electrolytes 0.17 M NaCl and 1 M Na_2SO_4 (Merck) of analytical grade and 2×10^{-4} M of BR46 and BY28 dye was prepared and used in all experiments. A universal buffer of pH 2 (0.04 M per 1 L) was prepared as recommended by Britton and Robinson (Britton, 1952). All aqueous preparations were performed using deionized water. All reagents were used as received without further purification.

2.2 Instruments

GW Laboratory DC power supply (GPC-6030D) was used as a source of DC electric current. Electrical cables connected both anode and cathode electrodes to DC power supply terminals. Spectrophotometric measurements were performed using the Thermo Fisher Scientific model EVO 60 spectrophotometer. The pH values of the solutions were measured using the Jenway 3505 pH meter before and after the electrochemical treatment. A RADWAG Wagi Elektroniczne sensitive analytical balance of model AS220/C/1 with 0.0001 g precision was used. FT-IR spectra were recorded using a Thermo Electron Corporation spectrometer (Madison, WI53,711, USA), scanned over a range of 4000–400 cm^{-1} at a spectral resolution of $2 \pm cm^{-1}$ using the KBr disk technique. The GC instrument equipped with an HP-5MS column (30 m $\times$ 0.25-mm internal diameter and 0.25-µm film thickness) was used for chromatographic gas analyses, as previously mentioned by Zayed et al. (Belal et al., 2022). A silylation reagent was used to convert volatile compounds to nonvolatile ones, which can respond to the GC-MS temperature gradient. The cyclic voltammetric (CV) measurements were performed using an Autolab potentiostat/

galvanostat model PGSTAT302N (Metrohm Autolab, Utrecht, Netherlands), employing the electrochemical NOVA 2.1.4 software. CV experiments were carried out at an ambient temperature of 25 °C $\pm$ 1 using a modified IrO_2/Ti electrode, graphite electrode, and 3.5 M KCl Ag/AgCl electrode as working, counter, and reference electrodes, respectively. The solution was purged with N_2 gas to remove the oxygen from the electrolyte before (for 10 min) and during CV measurements. The electrodes used in the present study have an effective area of 1.9 cm^2 and they were graphite, platinized titanium, and IrO_2/Ti-modified electrodes as anodes; the cathode was a graphite electrode. The preparation of IrO_2/Ti-modified electrode was described in a similar manner by Abdel Ghany et al. (Awad & Ghany, 2015; Nabil, 2003).

2.3 Procedures

The electrochemical experiments were carried out in a Pyrex electrochemical cell with a networking volume of 60 mL electrolyte. In deionized water, the electrolyte constituents were BR46 textile dye, buffer solution, NaCl, and/or Na_2SO_4. The electrochemical experiments were performed for 60 min. IrO_2/Ti-modified electrode and graphite electrode were used as anode and cathode, respectively, and were immersed into the electrolyte at the same distance (2.5 cm) from opposite sides of the cell. The construction of the electrochemical reactor was illustrated by Zayed et al. (Belal et al., 2021). During the electrochemical experiments, 2 mL of the electrolyte solution was taken out at a definite time for UV-Vis spectral analysis, COD, and TOC measurements. The decolorization percentage (color removal percentage) was calculated using the equation.

$$\text{Color removal}(\%) = 100(A_0 - A_t)/A_0 \quad (1)$$

where A_0 is the initial absorbance at the selected wavelength and A_t is the absorbance at time t at the selected wavelength. The measurements were taken at wavelength 530 nm for BR46 and 440 nm for BY28. For measurement consistency purposes, most of the measured values were repeated five times and statistically processed.

The solution of binary dyes mixture with a total concentration of 2×10^{-5} M was prepared from stock solutions of BY28 and BR46 in a concentration ratio of 2:1, 1:1, and 1:2 of BY28:BR46. The prepared binary dye solution was then added to the supporting electrolyte mixture of Na_2SO_4 and NaCl, and either the pH of the prepared solutions was 5.5 (without pH adjustment) or the pH was adjusted by adding a universal buffer solution to reach 2.0.

2.4 Analyses and Calculations

The COD and TOC values were measured before and after the electrochemical treatment. COD measurements were done as described in standard ISO 15705-2002 (Water quality - Determination of the chemical oxygen demand index (ST-COD) Small-scale sealed-tube method) (Belal et al., 2021). TOC measurements were performed using Multi N/C 2100S TOC apparatus (Analytik Jena, Germany) (Belal et al., 2022). The extent of COD and TOC removal values was calculated using Eq. (2) and Eq. (3).

$$\text{COD Removal} \% = 100 \left(COD_0 - COD_t\right)/COD_0 \quad (2)$$

$$\text{COD Removal} \% = 100 \left(TOC_0 - TOC_t\right)/COD_0 \quad (3)$$

where COD_0 and TOC_0 are the values before the electrochemical treatment, while COD_t and TOC_t are the values after the electrochemical treatment.

Current efficiency and energy consumption parameters were calculated per gram of COD removed. Equations (3) and (4) were used to calculate current efficiency and energy consumption, respectively.

$$\text{Current Efficiency} = 100 \left[\left(COD_0 - COD_t\right)FV/8It\right] \quad (4)$$

$$\text{Energy Consumption} = UIt/3600 \left(COD_0 - COD_t\right)V \quad (5)$$

where COD_0 is the COD before electrolysis (g L^{-1}), COD_t is the COD after electrolysis (g L^{-1}), U is the voltage (V), and F is Faraday's constant (96,487C mol^{-1}).

I is the current applied (A), t is the electrolysis time (s), V is the volume (L), and 8 is the equivalent weight of oxygen.

3 Results and Discussion

3.1 Electrochemical Oxidation Parameters

Different parameters such as pH, current density, electrode material, dye, and electrolyte concentration were measured and used during the electrochemical oxidation process to study the degradation of BR46 textile dye electrochemically.

3.1.1 pH

The pH optimization plays an important role in the dye degradation; therefore, the pH effect over the range of 2–10 was studied to select the optimum one for the dye degradation. The obtained results are shown in Fig. 2. The universal buffer was used to overcome the observed change in pH during the treatment.

From the data presented (Fig. 2A), the decolorization of BR46 dye increases by decreasing the pH and is dependent upon the pH of the solution. The maximum decolorization was 92.7% at pH 2.0 after 15 min. The ionization degree of cationic dye is pH dependent. At an alkaline medium, the formation of a precipitated photochromic compound was detected. The hydroxyl radicals are highly generated at acidic pH, and the dye decolorization is enhanced. But at alkaline pH, electrolytes would be consumed excessively, and the conductivity of the solution would be reduced, causing retardation of dye degradation (Dai et al., 2013; Körbahti & Turan, 2016).

The results in Fig. 2B agrees with the results of Na_2SO_4 (Fig. 2A), which means that working under acidic pH is favored over working under alkaline or neutral pH. The decolorization percent was 92.2% at pH 2.0 after 15 min, while it was 86.8%, 73.9%, and 68.1% at pH 4, 7, and 10, respectively, after 60 min. The non-buffered (pH 5.5) solution achieved good

Fig. 2 Effect of pH on 2×10^{-5} M of BR46 mixed with 6.6×10^{-3} M of universal buffer and 0.08 M of Na_2SO_4 (**A**), or 0.03 M of NaCl (**B**), for 60 min, at 0.03 A cm^{-2}, 530 nm, and using IrO_2/Ti and graphite electrodes
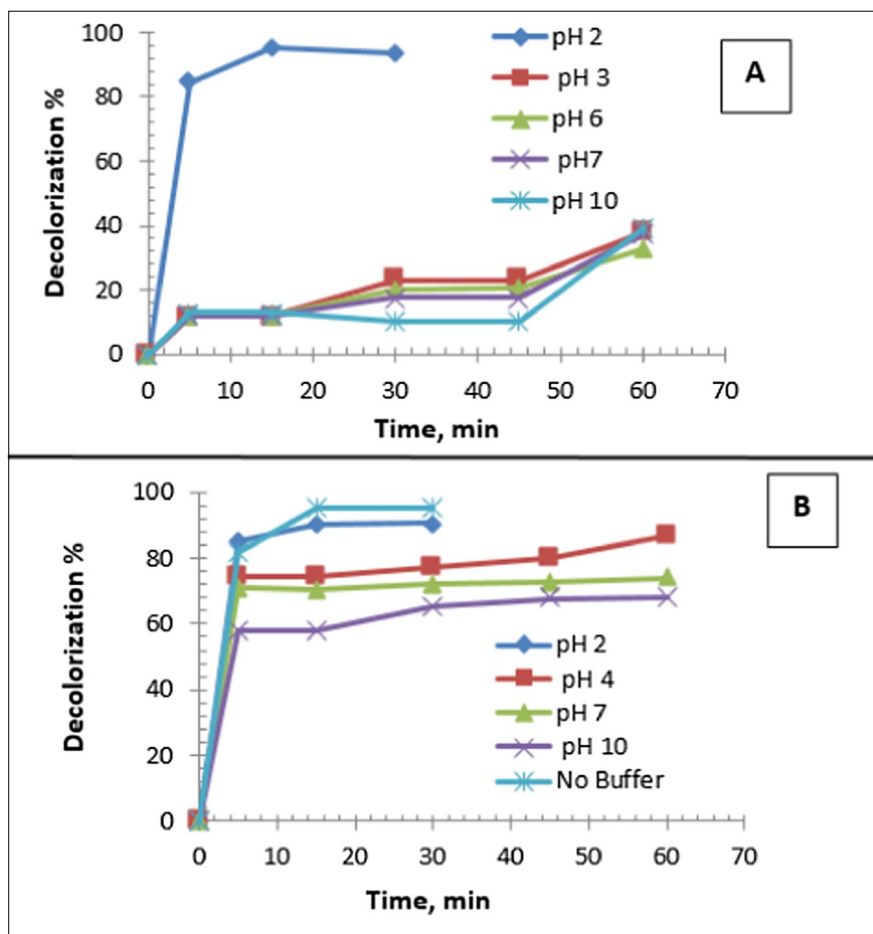
decolorization of % (94.4%) within 20 min with a little change in pH during the treatment.

The electrochemical degradation of BR46 occurs faster in acidic and neutral pH values than in the alkaline medium. It is due to Cl_2(aq) as a predominant species up to a pH close to 3 with $E° = 1.36$ V (vs. SHE). The HClO is the predominant one at the pH range between 3 and 8 with $E° = 1.49$ V (vs. SHE). These species have a higher standard potential than ClO^- which is predominant at pH above 8 with $E° = 0.89$ V (vs. SHE) (Amaterz et al., 2020; Baddouh et al., 2018, 2019). Therefore, working under an acidic medium is not ecologically acceptable (Mijin et al., 2012). Consequently, the optimum pH for BR46 degradation with high percent decolorization works under the non-buffered solution (pH 5.5). The results were in good corresponding with other pieces of literature (El-Sayed et al., 2014; Gözmen et al., 2009; Park, 2012).
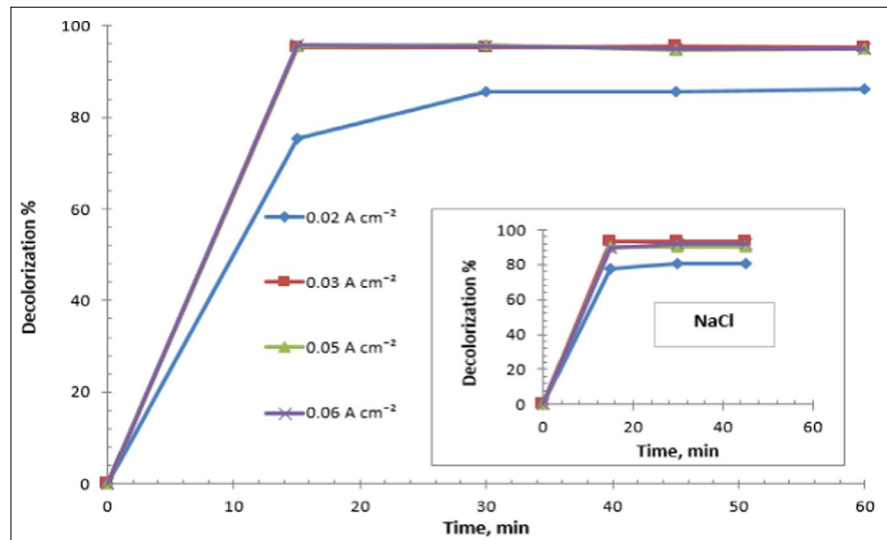
3.1.2 Current Density

The influence of current density on the degradation of BR46 is very similar in both electrolytes (Na_2SO_4, NaCl). Different current densities (0.02, 0.03, 0.05, and 0.06 A cm^{-2}) were applied to investigate its effect on dye degradation, and the results obtained are shown in Fig. 3.

The results presented in Fig. 3 refer to the increasing decolorization efficiency of the tested dye. The required time is shortened by increasing the applied current density due to forming more oxidants (OH·) (chlorine/hypochlorite).

At a current density greater than 0.03 A cm^{-2}, the degradation efficiency was slightly decreased due to the overpotential required for the generation of oxidants, which will be enhanced and consumed more energy (Yang et al., 2016). Also, an increase in oxygen evolution would compete with the degradation

Fig. 3 Different current densities of 2×10^{-5} M of BR46 mixed with 0.08 M of Na_2SO_4 and 6.6×10^{-3} M of universal buffer, at pH 2.0, for 60 min, 530 nm, and using IrO_2/Ti, graphite electrodes. Inset plots: using 0.03 M of NaCl as an electrolyte at pH ≈ 5.5


of organic substances (Kariyajjanavar et al., 2011a). Therefore, the optimal current density for BR46 degradation is 0.03 A cm^{-2}.

The presented values are the mean for five replicates. Their standard and relative standard deviations ranged from 0.016 to 0.078 and 0.58 to 0.98, respectively. The results were in a good corresponding with other literature (El-Sayed et al., 2014; Park, 2012).

3.1.3 Electrode Material Type

The material type of the anode electrode is one of the most operating factors influencing the efficiency of the electrochemical degradation of the dye. The meshed IrO_2/Ti (DSA) behavior was compared as a dimensionally stable anode with other conventional electrodes, of the same surface area (1.9 cm^2). Their effect on the decolorization of BR46 dye in the presence of either sodium sulfate or sodium chloride as supporting electrolytes are illustrated in Fig. 4.

From the results depicted in Fig. 4, it can be seen that all used electrodes achieved the complete decolorization of BR46 within 15 min. Nevertheless, meshed Ti-coated IrO_2-modified electrode had the best decolorization percentage (92.7%) and (94.0%) by using Na_2SO_4 and NaCl, respectively, than meshed Ti-coated Pt or graphite one. Due to the presence of the IrO_2 layer, the IrO_2/Ti-meshed electrode can maintain durability at a high current density for an extended period, thereby preventing the formation of an insulating titanium oxide layer
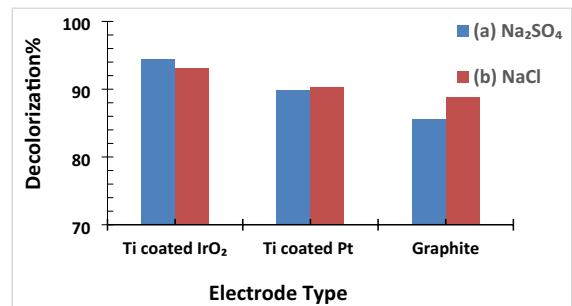
Fig. 4 Effect of electrode type against graphite electrode as a cathode on 2×10^{-5} M of BR46 mixed with 0.08 M of Na_2SO_4 and 6.6×10^{-3} M of universal buffer at pH 2.0 (a), 0.03 M of NaCl at pH ≈ 5.5 (b), for 60 min, 0.03 A cm^{-2}, and 530 nm

between the electrocatalytic active substances and the Ti substrate during the electrolysis. This electrode is therefore preferred over a pure Ti electrode. It also has economic advantages over Pt electrodes. Besides, Pt, IrO_2, and RuO_2 are known to function as active metal oxide (MO) anodes. At high O_2 overvoltages, the initial water oxidation on these MOs yields physisorbed MO_x(OH•) via reaction (6), which can be followed by its oxidation to chemically adsorbed "superoxide" MO_{x+1} by reaction (7). At the active MO anode surface, MO_{x+1} is generated to a greater extent than MO_x(OH•); therefore, the organic matter would be oxidized to relatively low mineralization (Awad & Ghany, 2015; Isarain-Chávez et al., 2017):

$$MO_x + H_2O \rightarrow MO_x(OH\bullet) + H^+ + e^- \qquad (6)$$

$$MO_x(OH\bullet) \rightarrow MO_{x+1} + H^+ + e^- \qquad (7)$$
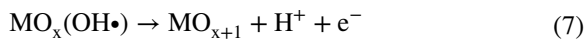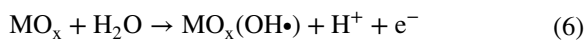
The explanation above proves the excellent catalytic activity of IrO$_2$/Ti electrode in organic dyes degradation (Belal et al., 2021). The results were in a good corresponding with other literature (Gözmen et al., 2009).

3.1.4 Initial Dye Concentration

The influence of initial dye concentration over the range of $(1–5)\times10^{-5}$ M was investigated, and the results are shown in Fig. 5.

The results in Fig. 5 show that all tested concentration ranges of BR46 dye exhibit decreasing in the absorbance within 20 min using Na$_2$SO$_4$ or NaCl, indicating the dye degradation and that the values of decolorization percentage were converged. These

Fig. 5 Effect of initial dye concentration $(1–5)\times10^{-5}$ M of BR46 mixed with 0.08 M of Na$_2$SO$_4$ and 6.6×10^{-3} M of universal buffer at pH 2.0 (**a**), 0.03 M of NaCl at pH ≈ 5.5 (**b**), for 60 min, at 0.03 A cm^{-2}, 530 nm, and using IrO$_2$/Ti, graphite electrodes
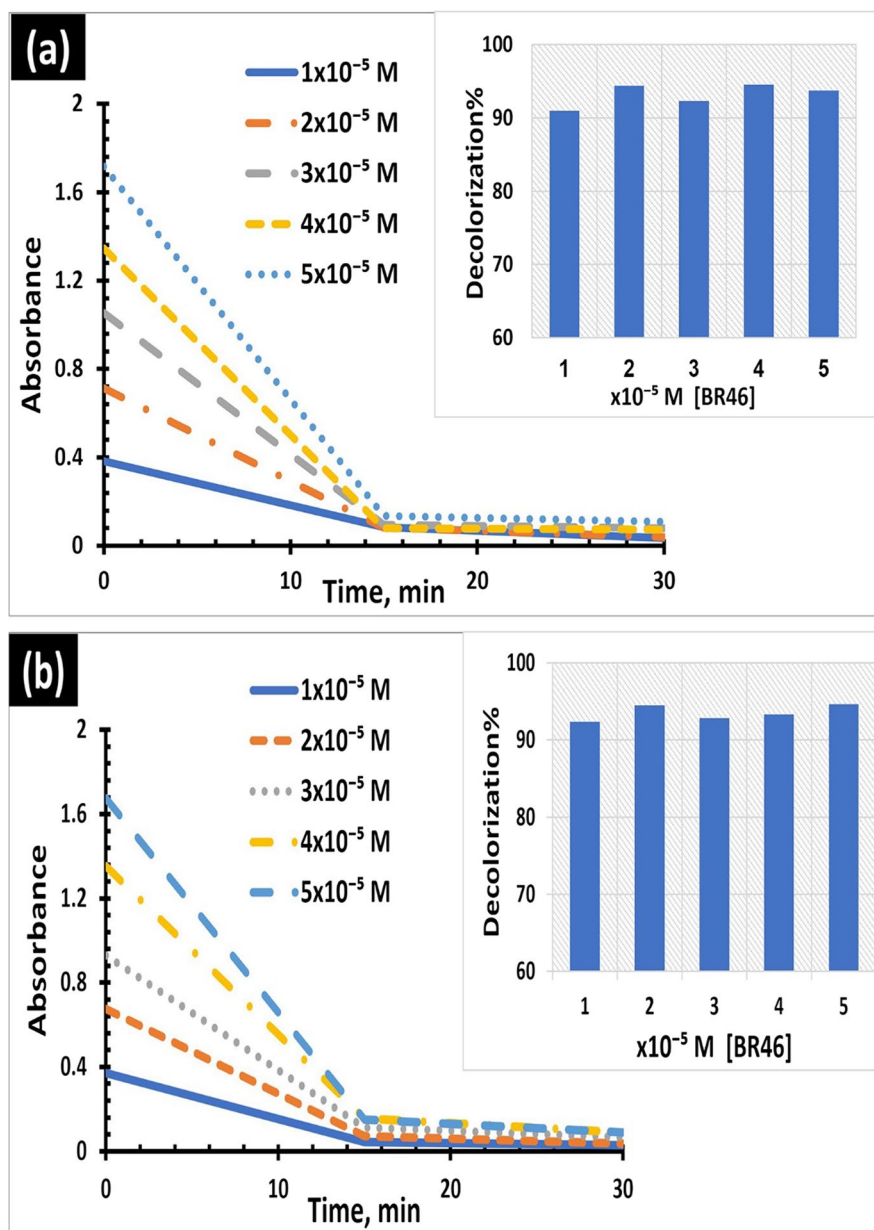
results confirm that the electrochemical degradation of BR46 dye was independent of the initial dye concentration. The presented values are the average of five replicates. Their standard and relative standard deviations ranged from 0.003 to 0.014 and 0.5 to 0.77 (Fig. 5a) and ranged from 0.022 to 0.08 and 0.42 to 0.71(Fig. 5b), respectively. The results were in a good corresponding with other pieces of literature (El-Sayed et al., 2014; Gözmen et al., 2009; Park, 2012).

3.1.5 Supporting Electrolyte Concentration

The concentration of sodium sulfate or sodium chloride as a supporting electrolyte on BR46 degradation was investigated, and the results are illustrated in Fig. 6.

From Fig. 6a, it is concluded that, for all the investigated Na_2SO_4 concentrations, the BR46 dye solutions were decolorized within 15 min. At the lowest concentration of Na_2SO_4 (0.04 M), the color removal rate was lower because of the reduction in the number of available electrolyte ions and hence the reduction of OH· radicals produced which led to an increase of the electrical resistance of the solution, followed by a reduction in the decolorization efficiency. Increasing the concentration of Na_2SO_4 up to 0.08 M would enhance the decolorization percentage to 92.3%. A further increase of the Na_2SO_4 concentration to 0.21 M would increase the production of $S_2O_8^{2-}$ and a drop in color abatement to 87.2% (Belal et al., 2021).

Based on Fig. 6b, it concluded that increasing the concentration of NaCl up to 0.03 M enhanced the decolorization percentage. Therefore, decolorization of 93.9% BR46 dye occurs after 20 min and at [NaCl] = 0.03 M. Further increase in NaCl concentration to greater than 0.03 M resulted in a drop in decolorization efficiency to reach 90.3% at [NaCl] = 0.06 M. This may be attributed to the accumulation of OCl^- which causes the pH increase and

Fig. 6 Effect of supporting electrolyte concentration on 2×10^{-5} M of BR46 mixed with Na_2SO_4 and 6.6×10^{-3} M of universal buffer at pH 2.0 (**a**), NaCl at pH ≈ 5.5 (**b**), for 60 min, at 0.03 A cm^{-2}, 530 nm, and using IrO$_2$/Ti, graphite electrodes
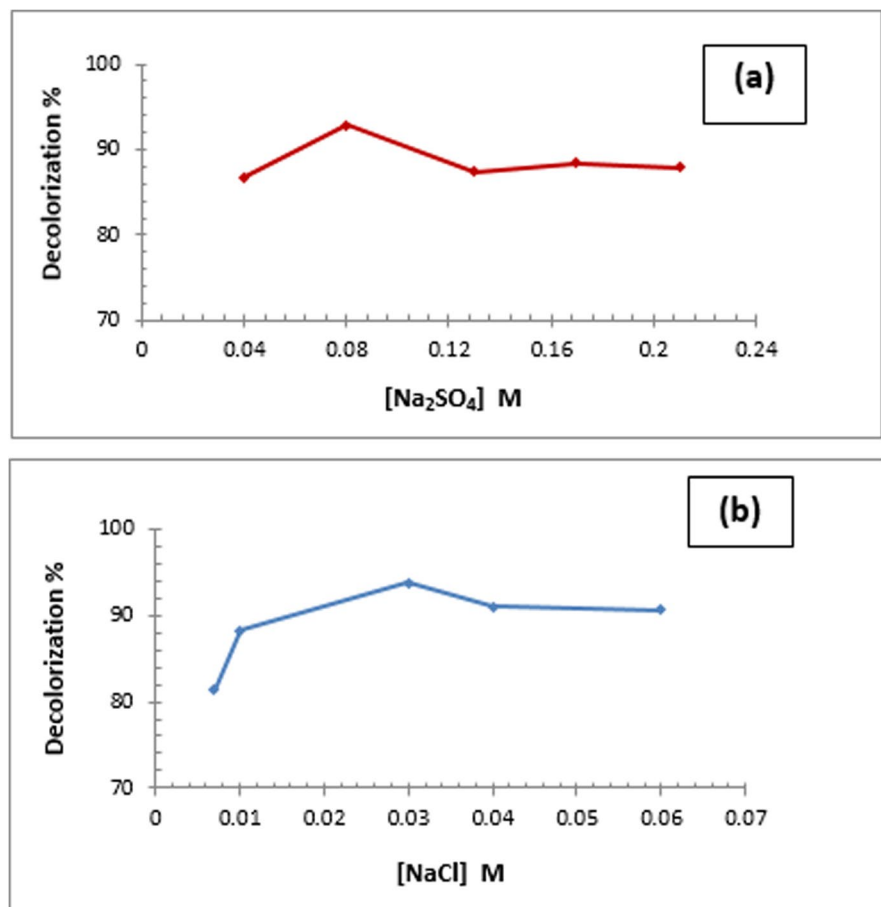
subsequently the formation of chlorate or perchlorate would be more dominant than the production of chlorine/hypochlorite (Hamad et al., 2018; Kariyajjanavar et al., 2011a). The presented values are the mean for five replicates. Their standard deviation and relative standard deviation ranged from 0.007 to 0.019 and 0.64 to 0.88 (Fig. 6a) and from 0.05 to 0.07 and 0.67 to 0.9 (Fig. 6b), respectively. The results were in a good corresponding with other pieces of literature (El-Sayed et al., 2014; Gözmen et al., 2009).

3.1.6 *Effect of Na₂SO₄ and NaCl Mixture as Supporting Electrolyte on Dye Degradation*

To increase the ionic conductivity of the BR46 reaction medium and to decrease the dye solution resistance, a mixture of sodium chloride and sodium sulfate supporting electrolyte was used.

3.2 Optimum Conditions of BR46 Dye Degradation

The effect of different concentrations of the mixed $NaCl + Na_2SO_4$ supporting electrolyte and pH on the decolorization of the BR46 dye was studied, and the results are shown in Fig. 7.

The data presented in Fig. 7 show the effect that four different concentrations (1) 0.007 M $NaCl + 0.02$ M Na_2SO_4, (2) 0.014 M $NaCl + 0.04$ M Na_2SO_4, (3) 0.03 M $NaCl + 0.08$ M Na_2SO_4, and (4) 0.04 M $NaCl + 0.13$ M Na_2SO_4 of the mixed

electrolyte have a great effect on the decolorization of the BR46 dye for three sets of conditions, marked as I, II, and III.

The data obtained at pH 2.0 with buffer solution are presented in Fig. 7 (I); it can be seen that the decolorization of BR46 has occurred in all tested mixed electrolyte concentrations within 15 min without a clear shift in decolorization percentage (91.9–94.2%).

Also, at pH 7.0 with buffer solution (Fig. 7 (III)), the decolorization occurred in all samples within 60 min. The decolorization percentage was increased with increasing mixed electrolyte concentration up to 0.03 M $NaCl + 0.08$ M Na_2SO_4 to reach 94.1%. A further increase of mixed electrolyte concentration (0.04 M $NaCl + 0.13$ M Na_2SO_4) would lead to a drop in decolorization percentage (91.8%) because of the accumulation of OCl^- and the production of $S_2O_8^{2-}$ (Belal et al., 2021; Hamad et al., 2018; Kariyajjanavar et al., 2011a).

As shown in Fig. 7 (II), in the absence of buffer and at pH 5.5, the decolorization occurred in all samples within 20 min. As the concentration of mixed NaCl and Na_2SO_4 increased, the decolorization time decreased, and the decolorization percentage increased (85.5–94.9%) up to a mixing electrolyte concentration of 0.03 M $NaCl + 0.08$ M Na_2SO_4. So it is considered the best results in energy consumption and working on a nearly neutral medium. A little development in the

Fig. 7 The effect of different concentrations of the mixed $NaCl + Na_2SO_4$ supporting electrolyte and pH on 2×10^{-5} M of BR46 in the presence of 6.6×10^{-3} M of universal buffer (at I, III only) for 60 min, at 0.03 A cm^{-2}, 530 nm, using IrO₂/Ti, graphite electrodes, where $\Omega = 0.5, 1, 2,$ and 3
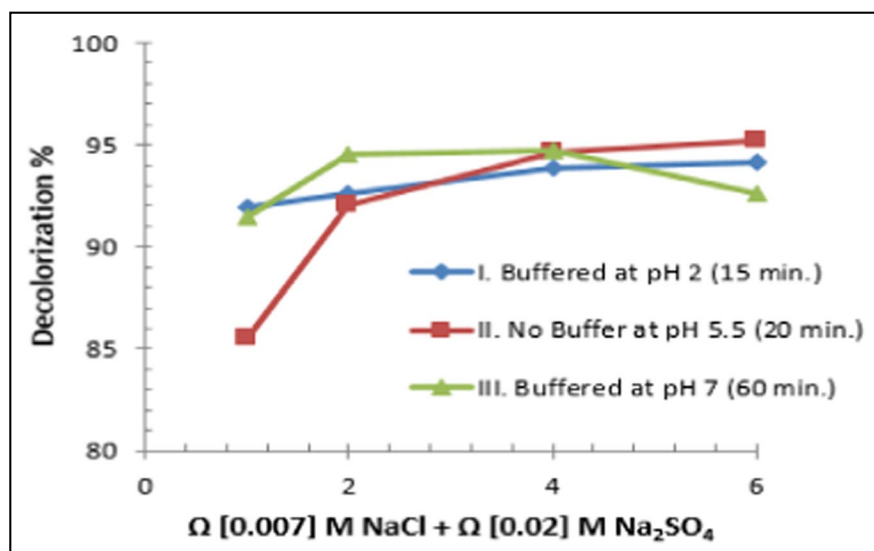
decolorization percentage (95.2%) was observed at 0.04 M NaCl + 0.13 M Na$_2$SO$_4$.

3.3 UV–Vis Spectrophotometric Mesurements

UV-visible spectrophotometer scanning was carried on before and after the electrochemical degradation of BR46 dye, using the selected proper pH conditions and concentration of mixing supporting electrolyte. The obtained results are illustrated in Fig. 8.

It can be concluded from Fig. 8 that after 20 min of the electrochemical treatment, BR46 dye is completely decolorized by the disappearance of the absorption band 530 nm. In contrast, the permanence of the absorption band 285 nm indicates the aromatic ring intermediates generation.

3.4 COD, TOC, Current Efficiency, and Energy Consumption Measurements

The extent of the degradation and mineralization of the dye as well as the validation of the proposed electrochemical process could be determined via COD, TOC, energy consumption, and current efficiency, respectively. Table 1 shows the results corresponding to the removal percentages of color, COD, and TOC in addition to the current efficiency and energy consumption values, calculated from the electrolysis of the BR46 dye by the modified Ti–IrO$_2$-meshed electrode using sodium sulfate and/or sodium chloride supporting electrolytes under proper conditions.

From Table 1, it can be seen that although the color removal % surpassed 92%, the COD and TOC removal % values did not surpass this value. This indicates the high refractory performance of the

Fig. 8 UV-visible spectra (before & after treatment) of 2×10^{-5} M of BR46 with mixture of 0.03 M NaCl and 0.08 M Na$_2$SO$_4$, at pH ≈ 5.5, 0.03 A cm^{-2}, and using IrO$_2$/Ti, graphite electrodes (A), BR46 dye in untreated and treated form (B)
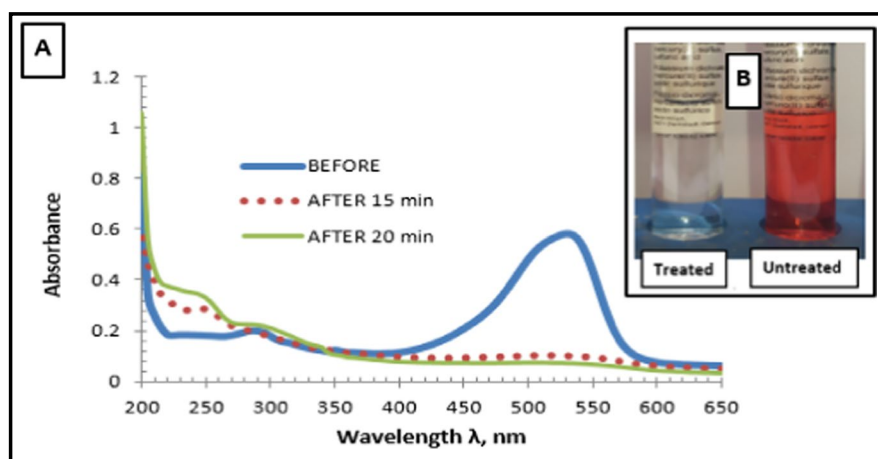
Table 1 Color, COD, and TOC removal %, and the current efficiency and energy consumption values for the electrochemical oxidation of BR46 dye (initial dye concentration 2×10^{-5} M, electrode area = 1.9 cm^2, electric current 0.06 A, and solution volume = 60 mL)

pH Before	pH After	Decolorization time, (min)	Color removal (%)	COD removal (%)	TOC removal (%)	Current efficiency (%)	Energy consumption (kWh (g COD)$^{-1}$))
1. Buffered 0.08 M Na$_2$SO$_4$ (Belal et al., 2021)							
2.0	2.1	15	92.7	34.3	66.6	54.3	37.0
2. Non-buffered 0.03 M NaCl (Belal et al., 2021)							
5.5	7.5	20	94.4	60.0	72.0	81.4	32.9
3. Mix. 0.03 M NaCl + 0.08 M Na$_2$SO$_4$, buffered							
2.0	2.1	15	93.8	39.7	63.7	67.0	27.0
7.0	7.2	60	94.1	42.5	60.8	79.7	25.2
4. Mix. 0.03 M NaCl + 0.08 M Na$_2$SO$_4$, non-buffered							
5.5	7.5	20	94.9	65.7	76.0	86.7	23.2

BR46 dye, whereas the loss of color of the BR46 dye does not indicate its complete mineralization. Only a fraction of the dye was completely oxidized into the water and carbon dioxide, as shown in the change in the TOC, while a significant fraction of the converted byproducts remained as a benzene ring, nitrogen-containing compounds, and soluble salts, as reflected in the changes in the COD (Mijin et al., 2012).

Also, the high current efficiency values are in complete agreement with the low energy consumption values. Performing the proposed treatment in the presence of NaCl as a supporting electrolyte shows preferable results than in Na_2SO_4 because the active anode (Ti–IrO_2) promotes the greater production of active chlorine, which attacks the organic molecules much more readily than hydroxyl radicals (Moreira et al., 2017; Panizza & Cerisola, 2009).

The best results are attained using a mixture of 0.03 M NaCl + 0.08 M Na_2SO_4 at pH≈ 5.5, where the color removal %, COD removal %, TOC removal %, current efficiency, and energy consumption were found to be 94.9%, 65.7%, 76.0%, 86.7%, and 23.2 kWh (g COD)$^{-1}$, respectively.

3.5 Cyclic Voltammetry Measurements

The electrolysis medium without the dye (blank) and with BR46 dye before and after electrochemical treatment is used in cyclic voltammetry to obtain preliminary information about the electrochemical process and to study its electroactive species. The redox reactions that take place between the surface of the IrO_2/Ti-modified electrode and the BR46 dye in the presence of a mixture of supporting electrolyte ($Na_2SO_4 + $ NaCl) via cyclic voltammetry are shown in Fig. 9.

Figure 9(a) shows the CV of blank; one anodic peak at + 0.698 V $II_p(A)$ in the forward scan and two cathodic peaks at − 0.332 V $I_p(C)$ and + 0.854 V $II_p(C)$ in the reverse scan were observed. The CV of the electrolysis medium in the presence of the dye (Fig. 9(b)) shows two anodic peaks at − 0.173 V $I_p(A)$ and + 0.836 V $II_p(A)$ in the forward scan and two cathodic peaks at − 0.297 V $I_p(C)$ and + 0.882 V $II_p(C)$ in the reverse scan. The BR46 dye in the presence of a mixture of Na_2SO_4 and NaCl would be considered reversible electrochemical nature, as $I_p(C)/I_p(A) \approx 1$ (Kariyajjanavar et al., 2011a).

The presence of a potential peak − 0.173 V $I_p(A)$ in the forward scan of Fig. 9(b) and its absence in Fig. 9(a) indicate the oxidation of BR46 dye. Also, the reduction in peak currents corresponding to $II_p(A)$ and $II_p(C)$ potential peaks in Fig. 9(b) confirms the dye oxidation. The presence of $II_p(A)$ potential peak as a shoulder may be due to the chlorine evolution process, which appears before the oxygen evolution reaction when NaCl is present in the solution (Szpyrkowicz et al., 2000).

The increase in peak current of $I_p(C)$ (Fig. 9(b)) than in (Fig. 9(a)) is due to the reduction of hypochlorite, which starts at − 0.4 V and would mask any other reduction peaks in cathodic and

Fig. 9 CV curves of mixture 0.03 M of NaCl and 0.08 M Na_2SO_4 without BR46 (a), and with 2×10^{-5} M of BR46 (b), at pH ≈ 5.5, using IrO_2/ Ti, graphite electrodes, the scan rate of 0.05 Vs^{-1}, and the potential window from + 1.0 V to − 1.0 V
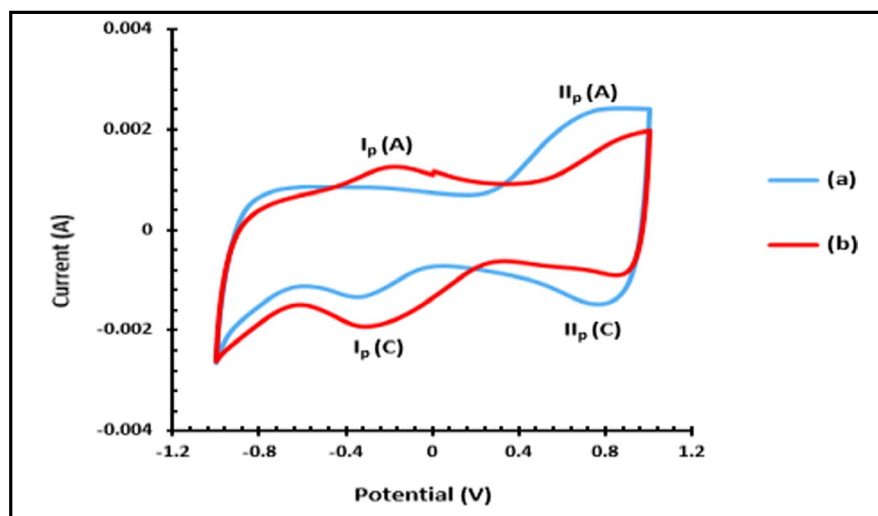
anodic direction (Mijin et al., 2012). The behavior of CV in the presence of a mixture of supporting electrolytes is more direct oxidation than indirect (Belal et al., 2022), confirming the powerful oxidizing activity of Cl⁻ than SO_4^{2-}. Therefore, the generation of active chlorine might reduce the generation of HO· when the electrode-applied current is limited (Li et al., 2013; Schümann & Gründler, 1998). The use of a mixture of Na_2SO_4 and NaCl as supporting electrolytes will oxidize BR46 dye with high efficiency in both direct and indirect one.

Also, the excellent electrocatalytic behavior of the IrO_2/Ti-modified electrode for the electrolysis of the cited dye was confirmed by successive cyclic scans (20 cycles), as shown in (Fig. 9(b)). There is no substantial change in the peak currents; therefore, surface passivation, which is responsible for diminishing the electroactive area and blocking the electrochemical response is not exist (Santos et al., 2016).

The extent of the degradation of BR46 dye with cyclic Voltammetry at different time intervals (0–20 min) at the proper conditions is shown in Fig. 10.

From the results presented in Fig. 10, it was found that $II_P(A)$ and $II_P(C)$ peak currents were reduced with time till electrolysis ended (after 20 min). Also, $I_P(A)$ was shifted to a more positive potential with the electrolysis time. These results demonstrated the degradation of BR46 dye into benzene ring intermediates (Kariyajjanavar et al., 2011a). In contrast, $I_P(C)$ current peak on the reduction side was found to be increased with electrolysis time due to the presence of inorganic anions such as Cl⁻, which formed during the dye degradation (Bhatnagar et al., 2014).

The effects of different scan rates in the range of 0.05–0.2Vs⁻¹ have great effects on the degradation of BR46 in the presence of the mixed NaCl and Na_2SO_4 supporting electrolyte, which was investigated, and the results are shown in Fig. 11.

Figure 11(I) shows the CV of different scan rates (from inner to outer: 0.05, 0.1, 0.15, 0.2 Vs⁻¹) and its effect on the dye electrolysis. As the scan rate increases, the peak current increases. A linear relationship between the redox current and the square root of the scan rate can be seen in Fig. 11(II).

The corresponding linear regression equation is $I_p(A) = 0.011\upsilon\,(Vs^{-1}) + 0.001$ with a correlation coefficient of 0.9955. This suggests that the redox process of the IrO_2/Ti electrode on organics is a diffusion mass transport mechanism followed by the product's adsorption. Also, it is observed that the difference between the anodic peak and cathodic peak potentials, ΔE_p, was increased with increasing scan rate (Jiang et al., 2020; Kariyajjanavar et al., 2011b; Santos et al., 2016).

3.6 FT-IR Spectroscopy Studies

FT-IR spectra were carried out before and after the electrochemical treatment of BR46 dye under the proper conditions to elucidate the functional groups of electrochemically degraded dye, as illustrated in Fig. 12.

From the previous IR chart, taking into consideration the redox reactions that take place and

Fig. 10 CV curves at different time intervals of the electrolysis of mixture 0.03 M of NaCl and 0.08 M Na_2SO_4 with 2×10^{-5} M of BR46, at pH ≈ 5.5, using Ti-IrO_2, graphite electrodes, the scan rate of 0.05 Vs⁻¹, and the potential window from + 1.0 V to − 1.0 V
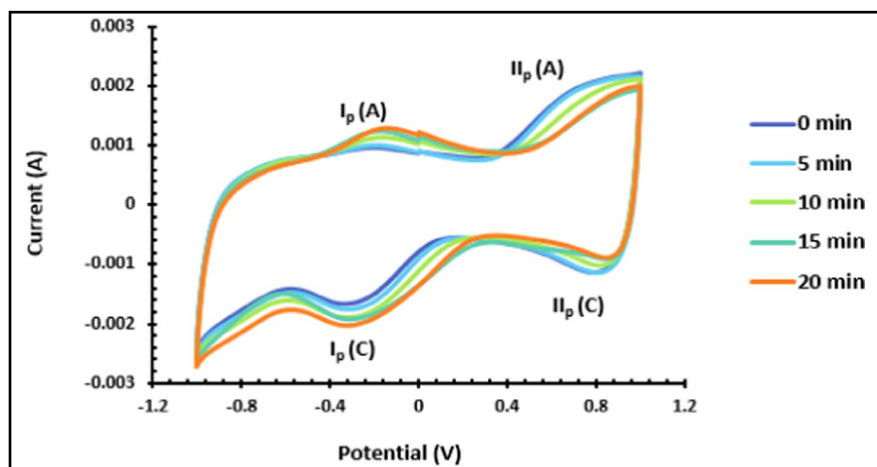
Fig. 11 CV curves of different scan rates of mixture 0.03 M of NaCl and 0.08 M Na$_2$SO$_4$ with 2×10^{-5} M of BR46, at pH ≈ 5.5, using IrO$_2$/Ti, graphite electrodes, the scan rate of 0.05 Vs^{-1}, and the potential window from $+1.0$ V to -1.0 V (I), linear relation between the peak currents and the square root of scan rates (II)
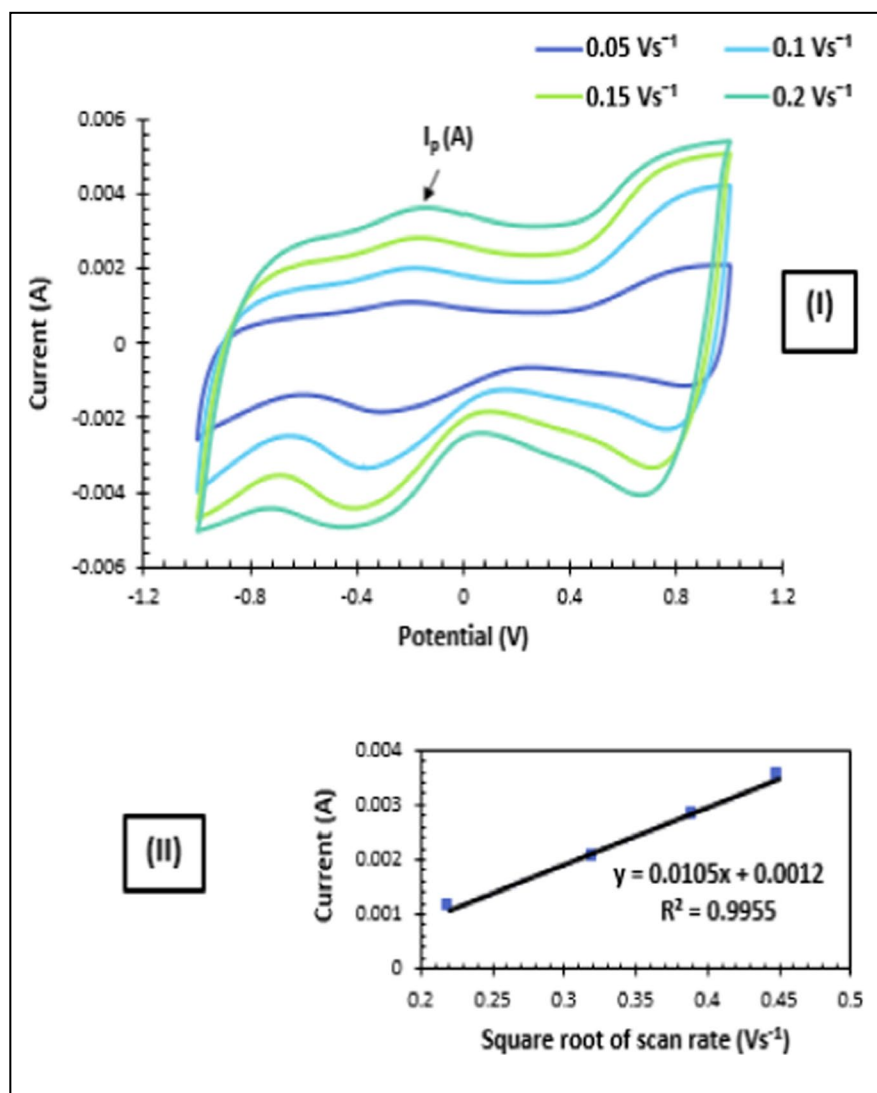

the elimination of the chromophore group as confirmed by the COD, TOC, and UV-Vis spectroscopy results, it is clear that there are two main bands present in all charts; a band I located at 3400 cm^{-1} and band II located at 1630 cm^{-1}. These two bands can be observed in the FT-IR spectrum of the BR46 dye before its electrochemical treatment but at lower intensities.

Band I appeared as a broad medium band before electrochemical treatment and become a sharper band with stronger intensity after the treatment and shifted from 3433 to 3439 cm^{-1}. Band II is also increased in the intensity after electrolysis, suggesting that the azo bond in the BR46 dye is opened

during the redox treatment and that its molecular configuration changes to a colorless non-conjugate structure from its original colored conjugate structure.

The low intensity of band II before the electrochemical treatment may be attributed to the possibility that an overlap exists between the bands associated with vibration modes of the aromatic ring and imine groups (C=N-) present in the tautomeric form of the azo group and secondary amides where the substituent of the N is an aromatic ring, and all of those present in the spectrum before electrolysis (Orts et al., 2018; Snehalatha et al., 2008; Socrates, 2004). The results verify the high refractory performance of
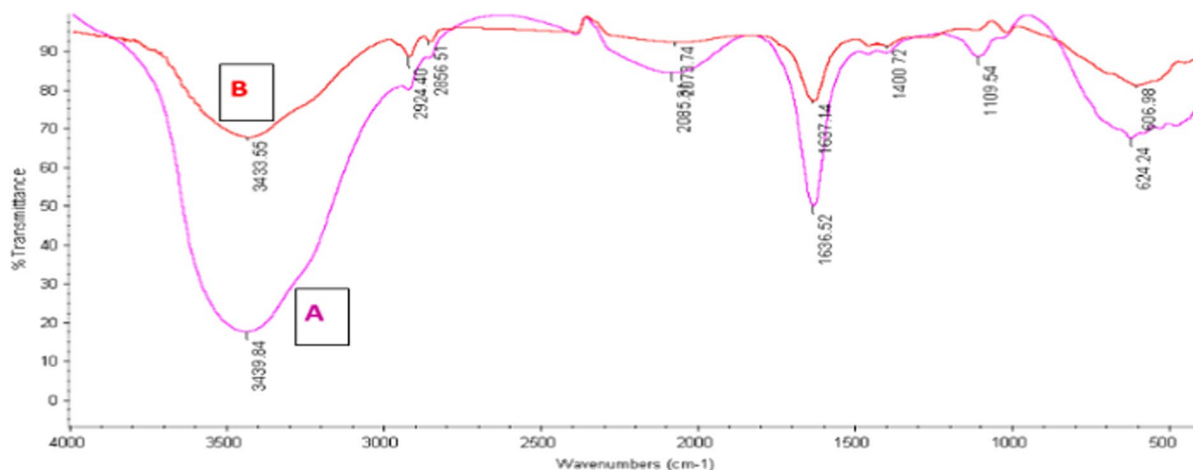
Fig. 12 FT-IR spectrum of 2×10^{-5} M BR46 dye before (B) and after (A) treatment in the presence of a mixture of 0.03 M NaCl and 0.08 M Na_2SO_4 at pH $\approx$ 5.5, using IrO_2/Ti, graphite electrodes, current density: 0.03 A cm^{-2}, time: 15 min

Fig. 13 Simple degradation pathway of BR46, confirmed by GC-MS
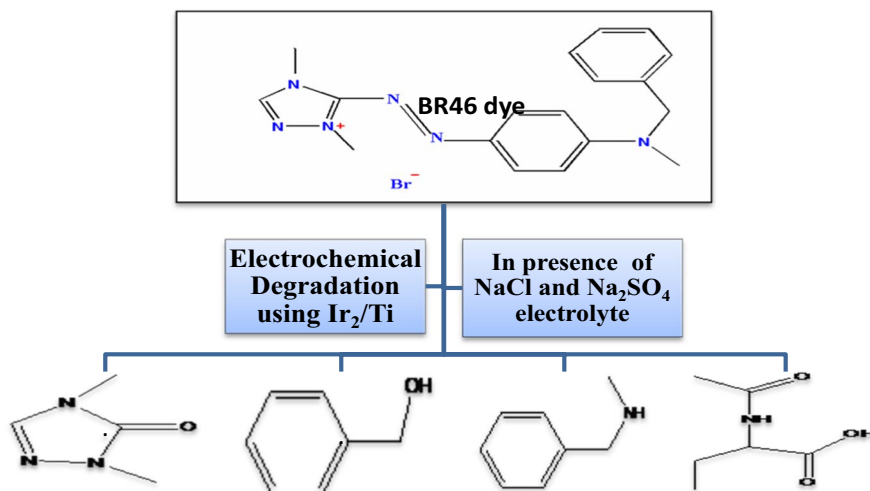
the BR46 dye, as confirmed by the significant fraction of byproducts remaining in the material.

3.7 GC–MS Spectra Studies

After the electrochemical treatment, GC-MS spectra of the BR46 dye solution were carried out to identify and elucidate the degradation products generated. The results can be summarized in Fig. 13 and Table 2.
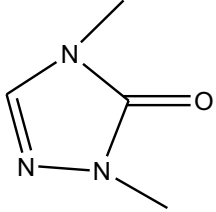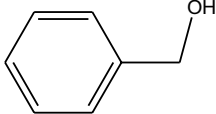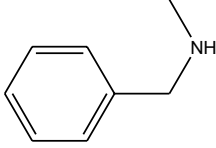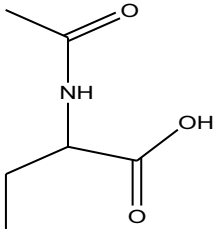
The data listed in Fig. 13 and Table 2 showed that five degradation products, which were generated from the electrochemical oxidation of BR46 dye solution by using IrO_2/Ti, had been successfully detected by GC-MS according to the library data. Several other chromatographic peaks were also found but could not be positively identified due to their formation at low concentration levels.

A supporting electrolyte mixture of NaCl and Na_2SO_4 was assumed to be preventing the production of any chlorinated byproducts always formed when active chlorine species contribute significantly to the oxidation of the dyes (Tavares et al., 2012).

About the formation of Hexane as a degradation product, it should be stated that due to the successive degradation of dye by various reactive oxygen species such as hydroxyl radicals, various linear organic compounds are produced with low molecular weights. Also, it may be formed when a radical

Table 2 The degradation products resulted from electrochemical degradation of BR46 dye solution by meshed IrO_2/Ti-modified electrode

No.	Compound Name	Molecular formula	t_R (min)	Main fragments (m/z)	Structure
1	2,4-Dimethyl-2,4-dihydro-[1,2,4]triazol-3-one	$C_4H_7N_3O$	21.334	126, 111, 97, 83, 70, 55, 41, 29	
2 [a]	Benzyl alcohol	C_7H_8O	24.035	165, 135, 91, 65	
3 [a]	N-Methylbenzylamine	$C_8H_{11}N$	26.547	193, 178, 164, 147, 135, 116, 91, 73, 59	
4 [a]	2-(Acetylamino) butanoic acid	$C_6H_{11}NO_3$	31.102	244, 202, 160, 100, 75	
5	Hexane	C_6H_{14}	37.241	106, 91, 78, 65, 39	

*[a]Value corresponding to the trimethylsilyl derivative

compound is generated as a product of the degradation process and its recombination with other produced degradation byproducts (Khataee et al., 2016).

The decomposition of the dye molecules to lesser colorless fragments of substituted aromatic compounds after the electrochemical treatment agreed with UV-Vis spectroscopy, COD, and TOC results. It confirmed the high refractory performance of the BR46 dye.

The electrochemical degradation pathway of BR46 was confirmed using GC-MS spectra. Four main components were produced in addition to hexane, which may be produced by a successive oxidation process. The main degradation pathways likely involve oxidative cleavage of the azo bonds (-N=N-) and aromatic rings. The -NH_2 groups on the dye may also be easily oxidized. Mineralization of smaller fragments then follows to produce CO_2, H_2O, and ions.

3.8 Investigations and Cyclic Voltammetry of Binary Mixture BY28 and BR46 Textile Dyes

Organic pollutants usually exist simultaneously in wastewaters; therefore, the studying of the electrochemical degradation and mineralization of a binary mixture of BY28 and BR46 textile dyes under the proper conditions is considered a point of concern.

3.8.1 UV–Vis Spectrophotometric

The electrochemical degradation of binary mixture solution textile dyes in the presence of a mixture of Na_2SO_4 and NaCl as supporting electrolytes and by using a meshed modified IrO_2/Ti electrode was scanned by UV-visible spectrophotometer to follow the degradation of textile dyes.

The UV-Vis spectra of different concentrations of a binary mixture of dyes at pH 5.5 were carried out before and after the electrolysis, as illustrated in Fig. 14.

The data presented in Fig. 14 show that all tested concentrations of a binary mixture of dyes were completely decolorized regardless of the initial concentration used and without interference, demonstrating the non-selectivity of active chlorine and hydroxyl radicals' strong oxidants. The decolorization was completely attained after 20 min.

The destruction of an azo group to nitrogen $(–N=N–)$ or $(–C=N–)$ double bond to carbon and nitrogen is the most active site for the oxidative attack of azo groups of dyes by the strong oxidant. This possibility is confirmed by the disappearance of absorption bands 440 nm and 530 nm of BY28 and BR46, respectively, resulting in complete decolorization of the binary mixture solution of the dyes. The obtained results are illustrated in Fig. 15, which shows the complete color removal of both binary dye mixture and single-dye solutions.

Fig. 14 UV-visible spectra (before & after treatment) of different concentrations of binary mixture solution of BY28 and BR46 dyes in the presence of a mixture of 0.03 M NaCl and 0.08 M Na_2SO_4, at 0.03 A cm^{-2}, using IrO_2/Ti, graphite electrodes, and at pH ≈ 5.5 (The inset presents the spectra of BR46 and BY28 in a single solution at the same conditions)
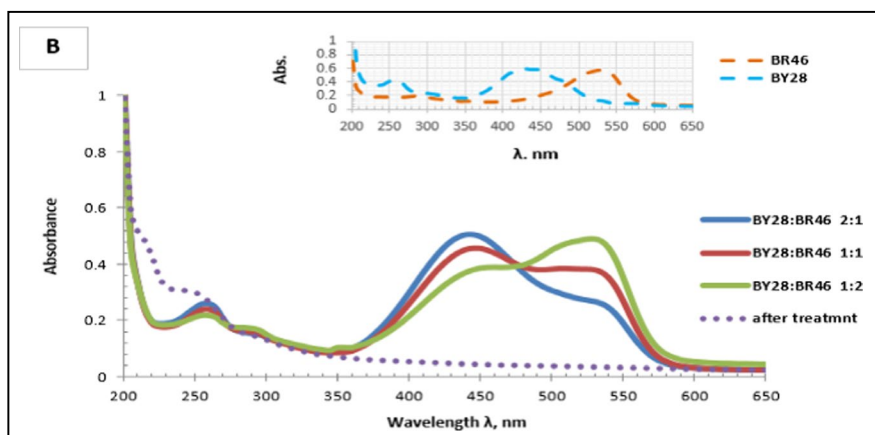
Fig. 15 The complete decolorization of binary dye's mixture and single-dye solutions
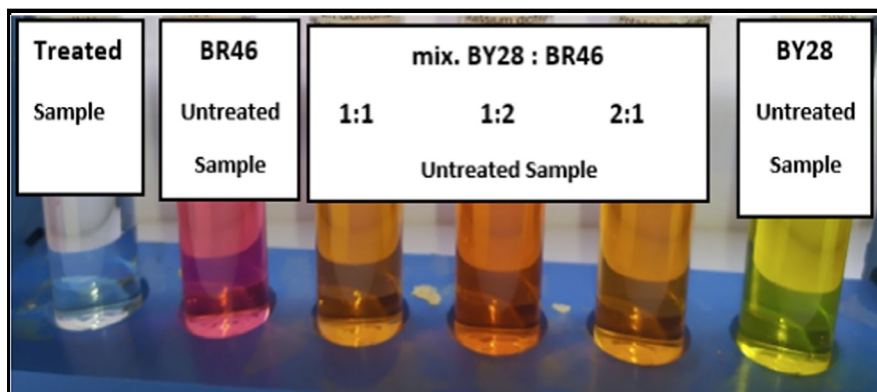
3.8.2 COD and TOC Measurements for Mixture BY28 and BR46 Dyes

The degree of degradation and mineralization can be determined by the abatement in COD and TOC values. The results corresponding to the removal percentages of COD and TOC, calculated from the electrolysis of a binary mixture of BY28 and BR46 dyes, were compared with those of a single solution of BY28 and BR46, as shown in. Figure 16

It can be clearly seen from the results in Fig. 16 that no significant change was observed between the binary or single solutions of dyes in the COD and TOC values. The COD % removal was 72.1% and 65.7% for a single solution of BY28 and BR46 dye, respectively, while it reached 70.0% in binary solutions of dyes. Also, the TOC % removal was 73.5% and 76.0% for the single solution of BY28 and BR46 dye, respectively, and 75.2% in binary dyes. It confirms that the extent of degradation and mineralization were similar in both binary and single solutions of BY28 and BR46 dyes.

3.8.3 Cyclic Voltammetry for Dyes' Mixture

The electrochemical processes occurring at the surface of the DSA electrode (IrO_2/Ti) by the organic compounds of a binary mixture of BY28 and BR46 textile dyes were explained via cyclic voltammetry. The CV experiments were performed as illustrated in Fig. 17.

Figure 17 shows that using different concentrations ratios of a binary mixture of BY28 and BR46 dyes did not affect the redox process on the electrode surface. CV data correlated well with UV-vis, COD, and TOC measurements, confirming that the solution of the binary dye mixture was degraded similarly to the single-dye solutions.

The cyclic voltammogram of concentration ratio 1:1 of BY28:BR46 binary mixture was taken as an example to describe the redox reaction that took place on IrO_2/Ti-modified electrode. The results obtained are presented in Fig. 18.

Figure 18(A) shows the CV of blank; one anodic peak at $+0.698$ V $II_p(A)$ in the forward scan and two cathodic peaks at -0.332 V $I_p(C)$ and $+0.854$ V $II_p(C)$ in the reverse scan were observed. The CV of the electrolysis medium in the presence of binary dyes mixture before the electrochemical treatment (Fig. 18(B)) shows one anodic peak at $+0.747$ V $II_p(A)$ in the forward scan and two cathodic peaks at -0.397 V $I_p(C)$ and $+0.718$ V $II_p(C)$ in the reverse scan.

Figure 18(C) shows the CV of the electrolysis medium in the presence of binary dyes mixture after the electrochemical treatment, two anodic peaks at -0.205 V $I_p(A)$ and $+0.806$ V $II_p(A)$ in the forward scan and two cathodic peaks at -0.350 V $I_p(C)$ and $+0.864$ V $II_p(C)$ in the reverse scan were observed. The binary mixture of BY28 and BR46 dyes would be considered a reversible electrochemical nature, as $II_p(C)/II_p(A) \approx 1$

Fig. 16 COD % and TOC % removal for the electrochemical oxidation of different concentrations of a binary mixture of BY28 and BR46 dyes and a single solution of 2×10^{-5} M of BR46 or BY28 dye, using the modified Ti–IrO_2-meshed electrode in the presence of a mixture of 0.03 M NaCl and 0.08 M Na_2SO_4, at 0.03 A cm^{-2}, and pH ≈ 5.5
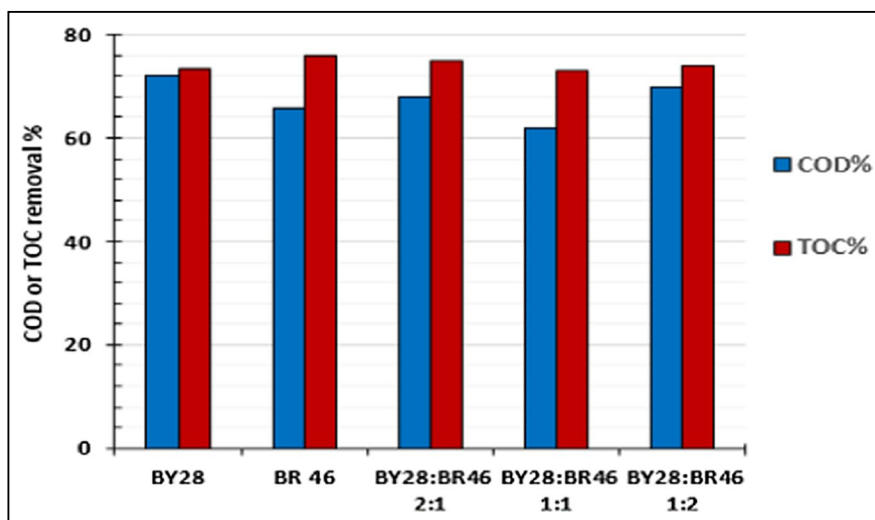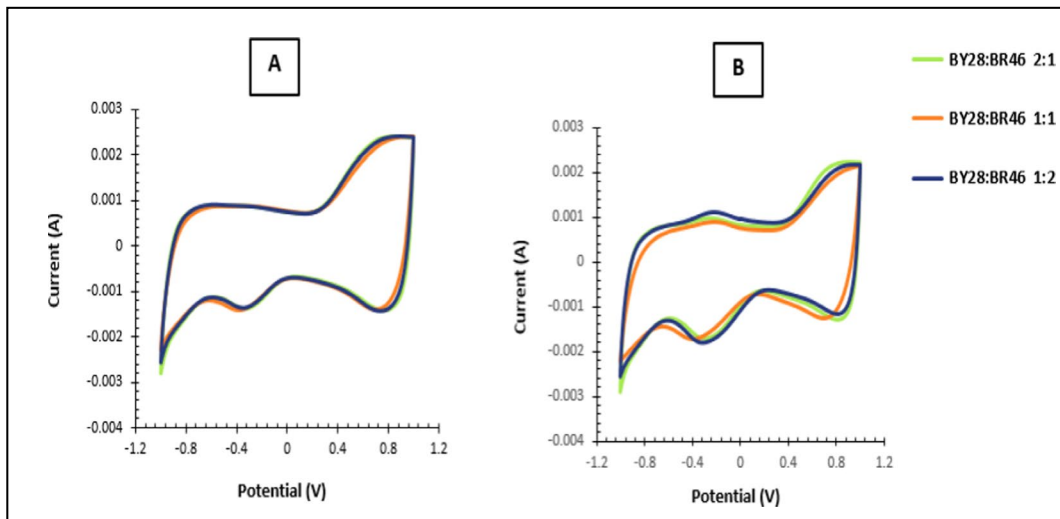
Fig. 17 CV curves of different concentrations ratio of a binary mixture of BY28 and BR46 dyes in the presence of a mixture of 0.03 M NaCl and 0.08 M Na$_2$SO$_4$, at pH ≈ 5.5, using IrO$_2$/ Ti, graphite electrodes, the scan rate of 0.05 Vs^{-1}, and the potential window from + 1.0 to − 1.0 V. (A) Untreated solutions. (B) Treated solutions

Fig. 18 CV curves of mixture 0.03 M of NaCl and 0.08 M Na$_2$SO$_4$ without binary dyes mixture (A), with 2×10^{-5} M of a binary mixture of BY28 and BR46 dyes before the electrochemical treatment (B), and after the electro-chemical treatment (C) at pH ≈ 5.5, using IrO$_2$/Ti, graphite electrodes, the scan rate of 0.05 Vs^{-1}, and the potential window from + 1.0 to − 1.0 V
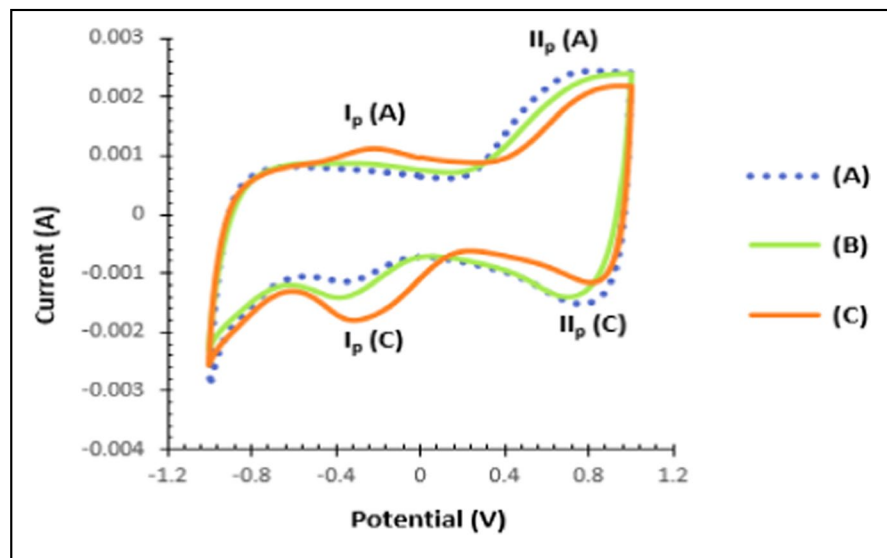
(Kariyajjanavar et al., 2011a). The presence of a potential peak − 0.205 V I$_p$(A) in the forward scan of Fig. 18(C) and its absence in both Fig. 18(A) and Fig. 18(B) indicates the oxidation of the binary mixture. Also, the reduction in peak currents and the shifting to the more positive potential corresponding to II$_P$(A) and II$_p$(C) potential peaks at Fig. 18(C) confirm the binary dye mixture oxidation.

The presence of II$_p$(A) potential peak as a shoulder may be due to the chlorine evolution process, which appears before the oxygen evolution reaction when NaCl is present in the solution (Szpyrkowicz et al., 2000). The increase in peak current of I$_p$(C) (Fig. 18(C)) is due to the reduction of hypochlorite, which starts at − 0.4 V and would mask any other reduction peaks in the cathodic and anodic direction (Mijin et al., 2012).

4 Conclusion

In this study, the degradation of BR46 textile dye and its binary mixtures with BY28 textile dye were efficiently accomplished using a modified DSA Ti–IrO$_2$-meshed electrode within 15–20 min. From the results obtained, the following conclusions are obtained:

1- The optimum conditions for the proposed electrochemical degradation were a current density of 0.03 A cm^{-2} and an initial dye concentration of 2×10^{-5} M; the optimum supporting electrolyte concentration was a mixture of 0.08 M Na$_2$SO$_4$ and 0.03 M NaCl at operating pH of 5.5.

2- UV–Vis spectrophotometric measurements confirmed that the disappearance of the absorption peak at 530 nm, which is assigned to an n$\rightarrow\pi$* transition, indicates complete decolorization of the cited dye.

3- The proposed degradation treatment leads to improve color, COD, and TOC removal percentages, current efficiency, and energy consumption values to 94.9%, 65.7%, 76.0%, 86.7%, and 23.2 kWh (g COD)$^{-1}$, respectively.

4- The CV results revealed a reduction in the peak currents with time up until the completion of the electrolysis, which indicates the degradation of the BR46 dye. A linear relationship, with a correlation coefficient of 0.996, between the redox current and the square root of the scan rate suggests that the redox process of the studied dye on the Ti–IrO$_2$ electrode surface follows a diffusion mass transport mechanism followed by product adsorption.

5- FT-IR data showed that the decolorization of the dye does not lead to their complete mineralization, with just a fraction of them being wholly oxidized into water and carbon dioxide. In contrast, a fraction of the converted byproducts remained as a benzene ring, nitrogen-containing compounds, and soluble salts.

6- GC-MS results showed that the degradation products which resulted from the decomposition of the BR46 dye molecule by the proposed electrochemical treatment were 2,4-dimethyl-2,4-dihydro-[1,2,4]triazol-3-one, benzyl alcohol, N-methylbenzylamine, 2-(acetylamino) butanoic acid, and hexane.

7- CV data and UV-vis, COD, and TOC measurements of binary dye mixtures were in good correlation. They confirmed that the binary solution was degraded and mineralized to the same extent as the single-dye solutions.

Data Availability The manuscript has no associated data.

Declarations

Conflict of Interest The authors declare no competing interests.

References

Aksu, Z. (2005). Application of biosorption for the removal of organic pollutants: A review. *Process Biochemistry, 40*(3), 997–1026.

Ali, M. F., El Ali, B. M., & Speight, J. G. (2005). Handbook of industrial chemistry: Organic chemicals," Ch.8 Dyes: Chemistry and Applications, *1st edition*, *McGraw-Hill Education*.

Amaterz, E., Tara, A., Bouddouch, A., Taoufyq, A., Bakiz, B., Lazar, F., Gilliot, M., Benlhachemi, A., Bazzi, L., & Jbara, O. (2020). Hierarchical flower-like SrHPO$_4$ electrodes for the photoelectrochemical degradation of Rhodamine B. *Journal of Appled Electrochemistry, 50*(5), 569–581.

Aquino, J. M., Pereira, G. F., Rocha-Filho, R. C., Bocchi, N., & Biaggio, S. R. (2011). Electrochemical degradation of a real textile effluent using boron-doped diamond or β-PbO2 as anode. *Journal of Hazardous Materials, 192*(3), 1275–1282.

Awad, A. M., & Ghany, N. A. A. (2015). Electrochemical advanced oxidation of cosmetics waste water using IrO₂/Ti-modified electrode. *Desalination and Water Treatment, 53*(3), 681–688.

Azbar, N., Yonar, T., & Kestioglu, K. (2004). Comparison of various advanced oxidation processes and chemical treatment methods for COD and color removal from a polyester and acetate fiber dyeing effluent. *Chemosphere, 55*(1), 35–43.

Baddouh, A., Bessegato, G. G., Rguiti, M. M., El Ibrahimi, B., Bazzi, L., Hilali, M., & Zanoni, M. V. B. (2018). Electrochemical decolorization of Rhodamine B dye: Influence of anode material, chloride concentration and current density. *Journal of Environmental Chemical Engineering, 6*(2), 2041–2047.

Baddouh, A., Amaterz, E., Ibrahimi, B. E., Rguitti, M. M., Bazzi, L., Errami, M., & Tkach, V. (2019). Enhanced electrochemical degradation of a basic dye with Ti/Ru$_{0.3}$ Ti$_{0.7}$ O$_2$ anode using flow-cell. *Desalination and Water Treatment, 139*, 352–359.

Basic Red 46. (n.d.). http://www.worlddyevariety.com/basic-dyes/basic-red-46.html. Accessed 16 Jan 2021

Belal, R. M., Zayed, M. A., El-Sherif, R. M., & Abdel Ghany, N. A. (2022). Electrochemical degradation and degree of mineralization of the BY28 dye in a supporting electrolyte mixture using an expanded dimensionally stable anode. *Electrocatal, 13*, 26–36.

Belal, R. M., Zayed, M. A., El-Sherif, R. M., & Abdel Ghany, N. A. (2021). Advanced electrochemical degradation of basic yellow 28 textile dye using IrO₂/Ti meshed electrode in different supporting electrolytes. *Journal of Electroanalytical Chemistry, 882*, 114979.

Bhatnagar, R., Joshi, H., Mall, I. D., & Srivastava, V. C. (2014). Electrochemical oxidation of textile industry wastewater by graphite electrodes. *Journal of Environmental Science and Health, Part A, 49*(8), 955–966.

Bogoeva-Gaceva, G., Bužarovska, A., & Dimzoski, B. (2008). Discoloration of synthetic dyeing wastewater using polyaluminium chloride. *Gazi University Journal of Science, 21*(4), 123–128.

Bouafia-Chergui, S., Oturan, N., Khalaf, H., & Oturan, M. A. (2012). Electrochemical and photochemical oxidation of cationic dyes: A comparative study. *Current Organic Chemistry, 16*(18), 2073–2082.

Britton, H. T. S. (1952). *Hydrogen ions* (4th ed.). Chapman and Hall.

Cotillas, S., Llanos, J., Castro-Ríos, K., Taborda-Ocampo, G., Rodrigo, M. A., & Cañizares, P. (2016). Synergistic integration of sonochemical and electrochemical disinfection with DSA anodes. *Chemosphere, 163*, 562–568.

Dai, Q., Shen, H., Xia, Y., Chen, F., Wang, J., & Chen, J. (2013). The application of a novel Ti/SnO₂-Sb₂O₃/PTFE-La-Ce-β-PbO₂ anode on the degradation of cationic gold yellow X-GL in sono-electrochemical oxidation system. *Separation and Purification Technology, 104*, 9–16.

Dos Santos, A., Cervantes, F., & van Lier, J. (2007). Review paper on current technologies for decolourisation of textile wastewaters: Perspectives for anaerobic biotechnology. *Bioresource Technology, 98*(12), 2369–2385.

El-Sayed, G. O., Awad, M. S., & Ayad, Z. A. (2014). Electrochemical decolorization of Maxilon Red GRL textile dye. *International Research Journal of Pure and Applied Chemistry, 4*(4), 402–416.

Eswaramoorthi, S., Dhanapal, K., & Chauhan, D. (2008). *Advanced in textile waste water treatment: the case for UV-ozonation and membrane bioreactor for common effluent treatment plants in Tirupur, Tamil Nadu, India.*. Environment with People's Involvement & Co-ordination in India. Coimbatore, India.

Farhadian, M., Askari, N., & Razmjou, A. (2015). Removal of textile dye from aqueous solutions by nanofiltration process. *IJET, 1*(2), 43–52.

Fil, B. A., & Günaslan, S. (2022). Comparison of different anodes and investigation of energy consumption in the treatment of real wastewater by electrooxidation. *International Journal of Environmental Research, 16*(5), 79–87.

Fil, B. A., & Günaslan, S. (2023). Electrooxidation treatment of slaughterhouse wastewater: Investigation of efficiency of Ti/Pt anode. *Particulate Science and Technology, 41*(4), 496–505.

Fil, B. A., Günaslan, S., & Uzuner, S. (2022). Turbidity removal from pistachio processing wastewater by electrooxidation: Investigation of efficiency and energy consumption of Ti/MMO anode. *EEMJ, 21*(11), 1825–1834.

Frijters, C., Vos, R., Scheffer, G., & Mulder, R. (2006). Decolorizing and detoxifying textile wastewater, containing both soluble and insoluble dyes, in a full scale combined anaerobic/aerobic system. *Water Research, 40*(6), 1249–1257.

Ghaly, A. E., Ananthashankar, R., Alhattab, M., & Ramakrishnan, V. V. (2014). Production, characterization and treatment of textile effluents: A critical review. *Journal of Chemical Engineering and Process Technology, 5*(1), 1–18.

Ghany, N. A. A., Meguro, S., Kumagai, N., Asami, K., & Hashimoto, K. (2003). Anodically deposited Mn-Mo-Fe oxide anodes for oxygen evolutionin hotseawater electrolysis. *Materials Transactions, 44*(10), 2114–2123.

Ghoreishi, S. M., & Haghighi, R. (2003). Chemical catalytic reaction and biological oxidation for treatment of non-biodegradable textile effluent. *Chemical Engineering Journal, 95*(1), 163–169.

Gomes De Moraes, S., Sanches Freire, R., & Duran, N. (2000). Degradation and toxicity reduction of textile effluent by combined photocatalytic and ozonation processes. *Chemosphere, 40*(4), 369–373.

Gözmen, B., Turabik, M., & Hesenov, A. (2009). Photocatalytic degradation of Basic Red 46 and Basic Yellow 28 in single and binary mixture by UV/TiO₂/periodate system. *Journal of Hazardous Materials, 164*(2–3), 1487–1495.

Hamad, H., Bassyouni, D., El-Ashtoukhy, E. S., Amin, N., & Abd El-Latif, M. (2018). Electrocatalytic degradation and minimization of specific energy consumption of synthetic azo dye from wastewater by anodic oxidation process with an emphasis on enhancing economic efficiency and

reaction mechanism. *Ecotoxicology and Environmental Safety, 148*, 501–512.

Isarain-Chávez, E., Baró, M. D., Rossinyol, E., Morales-Ortiz, U., Sort, J., Brillas, E., & Pellicer, E. (2017). Comparative electrochemical oxidation of Methyl Orange azo dye using Ti/Ir-Pb, Ti/Ir-Sn, Ti/Ru-Pb, Ti/Pt-Pd and Ti/RuO$_2$ anodes. *Electrochimica Acta, 244*, 199–208.

Jiang, N., Wang, Y., Zhao, Q., & Ye, Z. (2020). Application of Ti/IrO$_2$ electrode in the electrochemical oxidation of the TNT red water. *Environmental Pollution, 259*, 113801.

Kariyajjanavar, P., Jogttappa, N., & Nayaka, Y. A. (2011a). Studies on degradation of reactive textile dyes solution by electrochemical method. *Journal of Hazardous Materials, 190*(1–3), 952–961.

Kariyajjanavar, P., Narayana, J., & Nayaka, Y. A. (2011b). Degradation of textile wastewater by electrochemical method. *Hydrology: Current Research, 2*(1), 1–7.

Keshmirizadeh, E., & Farajikhajehghiasi, M. (2014). Decolorization and degradation of Basic Blue 3 and Disperse Blue 56 dyes using Fenton process. *JACR, 8*(3), 81–90.

Khataee, A., Gohari, S., & Fathinia, M. (2016). Modification of magnetite ore as heterogeneous nanocatalyst for degradation of three textile dyes: Simultaneous determination using MCR-ALS, process optimization and intermediate identification. *Journal of the Taiwan Institute of Chemical Engineers, 65*, 172–184.

Körbahti, B. K., & Tanyolac, A. (2008). Electrochemical treatment of simulated textile wastewater with industrial components and Levafix Blue CA reactive dye: Optimization through response surface. *Journal of Hazardous Materials, 151*(2), 422–431.

Körbahti, B. K., & Turan, K. M. (2016). Electrochemical decolorization of Reactive Violet 5 textile dye using Pt/Ir electrodes. *Journal of the Turkish Chemical Society Section A: Chemistry, 3*(3), 229–246.

Li, Q., Zhang, Q., Cui, H., Ding, L., Wei, Z., & Zhai, J. (2013). Fabrication of cerium-doped lead dioxide anode with improved electrocatalytic activity and its application for removal of Rhodamine B. *Chemical Engineering Journal, 228*, 806–814.

Limade, R. O. A., Bazo, A. P., Salvadori, D. M. F., Rech, C. M., de Palma Oliveira, D., & de Aragão Umbuzeiro, G. (2007). Mutagenic and carcinogenic potential of a textile azo dye processing plant effluent that impacts a drinking water source. *Mutation Research/Genetic Toxicology and Environmental Mutagenesis, 626*(1–2), 53–60.

Massué, C., Pfeifer, V., Huang, X., Noack, J., Tarasov, A., Cap, S., & Schlogl, R. (2017). High-performance supported iridium oxohydroxide water oxidation electrocatalysts. *Chemsuschem, 10*(9), 1943–1957.

Mathur, N., Bhatnagar, P., & Bakre, P. (2005). Assessing mutagenicity of textile dyes from Pali(Rajasthan) using Ames bioassay. *Applied Ecology and Environmental Research, 4*(1), 111–118.

Mijin, D. Ž, Avramov Ivić, M. L., Onjia, A. E., & Grgur, B. N. (2012). Decolorization of textile dye CI Basic Yellow 28 with electrochemically generated active chlorine. *Chemical Engineering Journal, 204–206*, 151–157.

Moreira, F. C., Boaventura, R. A. R., Brillas, E., & Vilar, V. J. P. (2017). Electrochemical advanced oxidation processes: A review on their application to synthetic and real wastewaters. *Applied Catalysis B: Environmental, 202*, 217–261.

Morikawa, Y., Shiomi, K., Ishihara, Y., & Matsuura, N. (1997). Triple primary cancers involving kidney, urinary bladder, and liver in a dye worker. *American Journal of Industrial Medicine, 31*(1), 44–49.

Nam, S., & Tratnyek, P. G. (2000). Reduction of azo dyes with zero-valent iron. *Water Research, 34*(6), 1837–1845.

Nilsson, R., Nordlinder, R., Wass, U., Meding, B., & Belin, L. (1993). Asthma, rhinitis, and dermatitis in workers exposed to reactive dyes. *British Journal of Industrial Medicine, 50*(1), 65–70.

Oliveira, D. P., Carneiro, P. A., Sakagami, M. K., Zanoni, M. V. B., & Umbuzeiro, G. A. (2007). Chemical characterization of a dye processing plant effluent—identification of the mutagenic components. *Mutation Research/Genetic Toxicology and Environmental Mutagenesis, 626*(1–2), 135–142.

Orts, F., del Río, A. I., Molina, J., Bonastre, J., & Cases, F. (2018). Electrochemical treatment of real textile wastewater: Trichromy Procion HEXL®. *Journal of Electroanalytical Chemistry, 808*, 387–394.

Panizza, M., & Cerisola, G. (2009). Direct and mediated anodic oxidation of organic pollutants. *Chemical Reviews, 109*(12), 6541–6569.

Park, D. S. (2012). Fabrication of flow cell using carbon fiber and electrochemical decomposition characteristics for organic dyes. *Journal of Environmental Science International, 21*(11), 1371–1377.

Rahman, F. (2016). The treatment of industrial effluents for the discharge of textile dyes using by techniques and adsorbents. *Journal of Textile Science and Engineering, 6*(1), 242–250.

Rajabi, A. A., Yamini, Y., Faraji, M., & Nourmohammadian, F. (2016). Modified magnetite nanoparticles with cetyltrimethylammonium bromide as superior adsorbent for rapid removal of the disperse dyes from wastewater of textile companies. *Nanochemistry Research, 1*(1), 49–56.

Rasoulifard, M. H., Marandi, R., Majidzadeh, H., & Bagheri, I. (2011). Ultraviolet light-emitting diodes and peroxydisulfate for degradation of Basic Red 46 from contaminated water. *Environmental Engineering Science, 28*(3), 229–235.

Regti, A., Laamari, M. R., Stiriba, S. E., & El Haddad, M. (2017). Potential use of activated carbon derived from Persea species under alkaline conditions for removing cationic dye from wastewaters. *Journal of the Association of Arab Universities for Basic and Applied Sciences, 24*, 10–18.

Sanroman, M. A., Pazos, M., Ricart, M. T., & Cameselle, C. (2004). Electrochemical decolourisation of structurally different dyes. *Chemosphere, 57*(3), 233–239.

Santos, M. J. R., Medeiros, M. C., Oliveira, T. M. B. F., Morais, C. C. O., Mazzetto, S. E., Martínez-Huitle, C. A., & Castro, S. S. L. (2016). Electrooxidation of cardanol on mixed metal oxide (RuO$_2$-TiO$_2$ and IrO$_2$-RuO$_2$-TiO$_2$) coated titanium anodes: Insights into recalcitrant phenolic compounds. *Electrochimica Acta, 212*, 95–101.

Schümann, U., & Gründler, P. (1998). Electrochemical degradation of organic substances at PbO$_2$ anodes: Monitoring by continuous CO$_2$ measurements. *Water Research, 32*(9), 2835–2842.

Singh, S., Srivastava, V. C., & Mall, I. D. (2013). Mechanism of dye degradation during electrochemical treatment. *Journal of Physical Chemistry C, 117*(29), 15229–15240.

Snehalatha, M., Ravikumar, C., Sekar, N., Jayakumar, V. S., & Joe, I. H. (2008). FT-Raman, IR and UV-visible spectral investigations and *ab initio* computations of a nonlinear food dye Amaranth. *Journal of Raman Spectroscopy, 39*(7), 928–936.

Socrates, G. (2004). *Infrared and Raman characteristic group frequencies: Tables and charts* (3rd ed.). John Wiley and Sons Ltd.

Szpyrkowicz, L., Juzzolino, C., Kaul, S. N., Daniele, S., & de Faveri, M. D. (2000). Electrochemical oxidation of dyeing baths bearing disperse dyes. *Industrial and Engineering Chemistry Research, 39*(9), 3241–3248.

Talukdar, M. K. (2001). Noise pollution and its control in textile industry. *Indian Journal of Fibre & Textile Research, 26*(1–2), 44–49.

Tavares, M. G., da Silva, L. V. A., Sales Solano, A. M., Tonholo, J., Martínez-Huitle, C. A., & Zanta, C. L. P. S. (2012). Electrochemical oxidation of methyl red using Ti/Ru $_{0.3}$Ti $_{0.7}$O $_2$ and Ti/Pt anodes. *Chemical Engineering Journal, 204–205*, 141–150.

Torres, E., Bustos-Jaimes, I., & Le Borgne, S. (2003). Potential use of oxidative enzymes for the detoxification of organic pollutants. *Applied Catalysis B: Environmental, 46*(1), 1–15.

Torres-Luna, J. A., Giraldo-Gómez, G. I., Sanabria-González, N. R., & Carriazo, J. G. (2019). Catalytic degradation of real-textile azo-dyes in aqueous solutions by using Cu–Co/halloysite. *Bulletin of Materials Science, 42*(4), 1–10.

Tsantaki, E., Velegraki, T., Katsaounis, A., & Mantzavinos, D. (2012). Anodic oxidation of textile dyehouse effluents on boron-doped diamond electrode. *Journal of Hazardous Materials, 207–208*, 91–96.

Tüfekci, N., Sivri, N., & Toroz, İ. (2007). Pollutants of textile industry wastewater and assessment of its discharge limits by water quality standards. *Turkish Journal of Fisheries and Aquatic Sciences, 7*(2), 97–103.

Uliana, C. V., Garbellini, G. S., & Yamanaka, H. (2012). Electrochemical reduction of Disperse Orange 1 textile dye at a boron-doped diamond electrode. *Journal of Appled Electrochemistry, 42*(5), 297–304.

Wang, K., Wei, M., Peng, T., Li, H., Chao, S., Hsu, T., Lee, H., & Chang, S. (2010). Treatment and toxicity evaluation of Methylene Blue using electrochemical oxidation, fly ash adsorption and combined electrochemical oxidation-fly ash adsorption. *Journal of Environmental Management, 91*(8), 1778–1784.

Yang, H., Liang, J., Zhang, L., & Liang, Z. (2016). Electrochemical oxidation degradation of Methyl Orange wastewater by Nb/PbO$_2$ electrode. *International Journal of Electrochemical Science, 11*, 1121–1134.

Yaqub, A., Isa, M. H., Ajab, H., Kutty, S. R. M., Ezechi, E. H., & Farooq, R. (2018). Preparation of Ti/IrO$_2$ anode with low iridium content by thermal decomposition process: Electrochemical removal of organic pollutants in water. *Electrochemical Energy Technology, 4*(1), 1–5.

Zaharia, C., Suteu, D., Muresan, A., Muresan, R., & Popescu, A. (2009). Textile wastewater treatment by homogenous oxidation with hydrogen peroxide. *Environmental Engineering and Management Journal, 8*(6), 1359–1369.

Zaviska, F., Drogui, P., Blais, J. F., & Mercier, G. (2009). In situ active chlorine generation for the treatment of dye-containing effluents. *Journal of Appled Electrochemistry, 39*(12), 2397–2408.